OPEN

The Pharmacogenomics Journal (2016) 16, 375–387

www.nature.com/tpj

ORIGINAL ARTICLE

Interindividual variability of CYP2C19-catalyzed drug metabolism due to differences in gene diplotypes and cytochrome *P*450 oxidoreductase content

Y Shirasaka[1,5], AS Chaudhry[2,5], M McDonald[3], B Prasad[1], T Wong[1], JC Calamia[1], A Fohner[1], TA Thornton[4], N Isoherranen[1], JD Unadkat[1], AE Rettie[3], EG Schuetz[2] and KE Thummel[1]

Large interindividual variability has been observed in the metabolism of CYP2C19 substrates *in vivo*. The study aimed to evaluate sources of this variability in CYP2C19 activity, focusing on *CYP2C19* diplotypes and the cytochrome *P*450 oxidoreductase (POR). *CYP2C19* gene analysis was carried out on 347 human liver samples. CYP2C19 activity assayed using human liver microsomes confirmed a significant *a priori* predicted rank order for (S)-mephenytoin hydroxylase activity of *CYP2C19*17/*17* > **1B/*17* > **1B/*1B* > **2A/*17* > **1B/*2A* > **2A/*2A* diplotypes. In a multivariate analysis, the *CYP2C19*2A* allele and POR protein content were associated with CYP2C19 activity. Further analysis indicated a strong effect of the *CYP2C19*2A*, but not the **17*, allele on both metabolic steps in the conversion of clopidogrel to its active metabolite. The present study demonstrates that interindividual variability in CYP2C19 activity is due to differences in both CYP2C19 protein content associated with gene diplotypes and the POR concentration.

The Pharmacogenomics Journal (2016) **16,** 375–387; doi:10.1038/tpj.2015.58; published online 1 September 2015

INTRODUCTION

CYP2C19 is a member of the human drug-metabolizing family of cytochrome *P*450 enzymes that is encoded by the *CYP2C19* gene. It is a clinically important enzyme that plays a critical role in the metabolism and related drug–drug interactions of a variety of therapeutic agents, including proton pump inhibitors, antiepileptic agents, antiplatelet drugs and antidepressants.[1–3] Large interindividual variability has been observed in the metabolism of these drugs *in vivo*, with differences presumed to be due in part to inherited variation in the *CYP2C19* gene. Similar to several other human *P*450 family members, CYP2C19 activity is polymorphic, with sub-populations of poor metabolizers, intermediate metabolizers, extensive metabolizers and ultrarapid metabolizers.[4–6]

Multiple allelic variants in the *CYP2C19* gene have been described, with over 69 reported to date (http://www.cypalleles.ki.se/cyp2c19.htm, the last update was 8 September 2014). Many of these are derived from nonsynonymous single-nucleotide polymorphisms (nsSNPs) in the coding regions of the *CYP2C19* gene. Some of these genetic changes profoundly affect hepatic *CYP2C19* expression, with metabolic insufficiency arising from the absence of CYP2C19 protein accumulation. For example, homozygosity for the *CYP2C19*2A* (19154G > A; rs4244285) allele causes aberrant mRNA splicing, resulting in no detectable hepatic protein and a poor metabolizer phenotype.[7,8] In contrast, the *CYP2C19*17* (−806C > T; rs12248560) allele is associated with an increase in transcriptional activity that has been described as causing ultrarapid metabolism of CYP2C19 substrates.[9,10]

In a clinical study involving the proton pump inhibitors omeprazole and lansoprazole, a genotype-dependent increase in drug area under the concentration-time curve and intragastric pH was observed, resulting in a change in the healing rate of peptic ulcer, gastroesophageal reflux disease and/or the *Helicobacter pylori* eradication rate.[11,12] Another prominent example involves bioactivation of the antiplatelet drug clopidogrel by CYP2C19. *CYP2C19*2* carriers receiving the drug are at increased risk for recurring cardiovascular events such as myocardial infarction, cerebral stroke and stent thrombosis than are patients homozygous for the wild-type allele.[13–15] This difference in clinical outcome has been attributed to significantly lower blood levels of the active thiol metabolite of clopidogrel in patients carrying the *CYP2C19*2* allele.[13] In contrast, the *CYP2C19*17* allele has been associated with an enhanced efficacy of clopidogrel in reducing reoccurring cardiovascular events, risk of stent thrombosis and residual platelet aggregation, while increasing the risk of bleeding events.[16–18] Although not all clopidogrel study results are in agreement, the *CYP2C19*17* allele has also been associated with enhanced metabolism of several other drugs, including omeprazole, amitriptyline, voriconazole, mephenytoin, pantoprazole and escitalopam.[9,19–26]

There is only a limited understanding of the mechanistic basis for the *CYP2C19*17*-associated phenotype. The putative causal SNP is found in the promoter of the *CYP2C19* gene and ostensibly affects the binding of transcription factors that enhance gene transcription.[9] However, a recent paper reported no statistically significant difference in CYP2C19 enzyme activity

[1]Department of Pharmaceutics, School of Pharmacy, University of Washington, Seattle, WA, USA; [2]Department of Pharmaceutical Sciences, St. Jude Children's Research Hospital, Memphis, TN, USA; [3]Department of Medicinal Chemistry, School of Pharmacy, University of Washington, Seattle, WA, USA and [4]Department of Biostatistics, School of Public Health, University of Washington, Seattle, WA, USA. Correspondence: Professor KE Thummel, Department of Pharmaceutics, School of Pharmacy, University of Washington, H272 Health Sciences Building, Box 357610, Seattle, WA 98195-7610, USA.
E-mail: thummel@u.washington.edu
[5]These two authors contributed equally to this work.
Received 23 July 2014; revised 19 May 2015; accepted 23 June 2015; published online 1 September 2015

((S)-mephenytoin hydroxylation) in microsomes from livers with a heterozygous or homozygous *CYP2C19*17* genotype, compared with liver microsomes from homozygous wild-type livers, although directionality of the observed trend supported the hypothesis.[10] The *CYP2C19*2* and *CYP2C19*17* loci appear to be in linkage disequilibrium (LD), and thus one finds a mixed allelic diplotype in the population (that is, *CYP2C19*2/CYP2C19*17*) that has an uncertain phenotype.[26–28] With this in mind, and the lack of clarity regarding the exact functional consequences of the *CYP2C19*17* allele, we sought to characterize interindividual variability of CYP2C19-catalyzed drug ((S)-mephenytoin and clopidogrel) metabolism in a large set of human livers and determine its dependency on the *CYP2C19*2* and *CYP2C19*17* allelic variants, with special consideration of predicted diplotypes, as well as the specific content of the obligatory coenzyme, cytochrome *P*450 oxidoreductase (POR). We also assessed the contribution of rare *CYP2C19* variation together with clinical and other demographic variables to interindividual differences in hepatic microsomal enzyme activity.

MATERIALS AND METHODS

Chemicals and reagents

(S)-mephenytoin was purchased from Sigma-Aldrich (St Louis, MO, USA). 4-Hydroxymephenytoin-d_3 was purchased from Toronto Research Chemicals (Toronto, ON, Canada). Clopidogrel, 2-oxo-clopidogrel, clopidogrel active thiol metabolite and prasugrel were all kindly provided by Eli Lilly (Indianapolis, IN, USA) and the Daiichi Sankyo (Tokyo, Japan). Stable isotope labeled amino acids [$^{13}C_6^{15}N_2$]-lysine and [$^{13}C_6^{15}N_4$]-arginine were purchased from Pierce Biotechnology (Rockford, IL, USA). All other chemicals and general reagents were of analytical grade or better and were obtained from various commercial sources such as Cerilliant (Round Rock, TX, USA), Invitrogen (Carlsbad, CA, USA) or Applied Biosystems (Foster City, CA, USA).

Tissue samples

A total of 347 different human livers used in the present study consisted of 65 samples obtained from the University of Washington Human Liver Bank (Seattle, WA, USA), a resource established by a Program Project grant on Drug Interactions from the National Institutes of Health (P01-GM32165) and 282 liver samples from the St Jude Liver Resource at St Jude Children's Research Hospital (Memphis, TN, USA), a resource established by the Liver Tissue Procurement and Distribution System (National Institutes of Health National Institute of Diabetes and Digestive and Kidney Diseases Contract N01-DK92310) and by the Cooperative Human Tissue Network. The collection and use of these tissues for research purposes was approved by the Human Subjects Institutional Review Boards at the University of Washington and St Jude Children's Research Hospital. In both cases, all links between archived tissues and the original donors were destroyed to preserve anonymity and facilitate study execution. Additional details about the selection of livers and sample size and investigator blinding for sample analysis can be found in Supplementary Methods.

Genotyping and CYP2C19 exon sequencing

Genomic DNA from human livers was isolated by use of a DNeasy tissue kit. Genotyping of the *CYP2C19*2* (rs4244285) and *CYP2C19*17* (rs12248560) variants was performed according to the manufacturer's instructions using TaqMan SNP genotyping assays (Applied Biosystems). The detailed methods used for genotyping and exon sequencing are described in the Supplementary Methods.[29]

LD analysis

Pairwise LD was calculated and displayed using Haploview 4.2 software.[30] The D′, along with its corresponding logarithm of odds (LOD) score, and r^2 LD values were determined between rs3758581 (*CYP2C19*1A* or **1B*), rs4244285 (*CYP2C19*2*) and rs12248560 (*CYP2C19*17*) SNPs. The frequencies of other alleles were too low for meaningful LD analysis.

Liver microsomal preparations

Human liver microsomes (HLMs) were prepared using a modified version of previously described methods.[31,32] The detailed method used for HLM preparations is described in the Supplementary Methods. To generate pooled HLMs from the following homozygous diplotypes (*CYP2C19*1B/*1B*, *CYP2C19*2A/*2A* and *CYP2C19*17/*17*), an equal amount of microsomal protein from 115, 5 and 23 individual preparations, respectively, was combined. Total protein concentrations were determined by the BCA Protein Assay (Pierce, Rockford, IL, USA). Total microsomal *P*450 concentrations for each of the HLM pools were determined by difference spectroscopy of the carbon monoxide-complexed hemoprotein.[33]

CYP2C19 activity assay in HLMs

(S)-Mephenytoin hydroxylation activity phenotyping and kinetic analysis. Liver microsomal CYP2C19 metabolic activity profiling was conducted at (S)-mephenytoin concentrations of 20 μM (fivefold below reported K_m values). For each liver microsomal preparation, incubations were performed in triplicate in solutions containing 100 mM potassium phosphate buffer (KPi, pH 7.4) and final incubation volumes were 100 μl. (S)-mephenytoin and HLM (0.1 mg ml^{-1}) were preincubated for 10 min at 37 °C before reactions were initiated by adding NADPH (1 mM, final concentration). Reactions were terminated after 20 min by adding an equal volume of ice-cold acetonitrile containing 100 nM internal standard (d_3-4′-hydroxymephenytoin).

For the determination of kinetic parameters, CYP2C19-catalyzed (S)-mephenytoin 4′-hydroxylation was measured in triplicate over a range of substrate concentrations (1–400 μM), using pooled HLMs with the following homozygous diplotypes: *CYP2C19*1B/*1B*, **2A/*2A* and **17/*17*. All incubation conditions and sample workup were the same as that described above for HLM phenotyping. The concentrations of 4′-hydroxy (S)-mephenytoin in the incubations were quantified using a liquid chromatography–tandem mass spectrometry (LC-MS/MS) system (Supplementary Methods).

2-Oxo-clopidogrel formation kinetics. Incubation mixtures contained 0.25 mg ml^{-1} of diplotype-defined pooled HLM protein, 1% of a 100× concentrated dimethyl sulfoxide stock solution of clopidogrel (for final substrate concentrations of between 100 nM and 100 μM) and 20 mM ascorbic acid in 100 mM KPi buffer, pH 7.4, containing 100 mM of the hepatic carboxylesterase inhibitor, NaF (to 200 μl final incubation volume). The reaction rate at each substrate concentration was determined in triplicate. After 3 min of preincubation at 37 °C/70 r.p.m. in a water bath, the reactions were initiated by the introduction of an aqueous stock solution of NADPH (1 mM final concentration). Reactions were quenched after 5 min of incubation at 37 °C/70 r.p.m. by the addition of a 50% volume of ice-cold acetonitrile, containing 80 nM prasugrel as internal standard, and were then centrifuged to remove protein. Supernatants were analyzed by LC-MS/MS (Supplementary Methods).

Clopidogrel active metabolite (CAM) formation kinetics. Incubation mixtures again contained 0.25 mg ml^{-1} microsomal protein, from one of the three *CYP2C19* diplotyped HLM pools, 1% of a freshly prepared 100× concentrated dimethyl sulfoxide stock solution of 2-oxo-clopidogrel (100 nM to 100 μM final concentration) and 20 mM ascorbic acid (included as a glutathione surrogate in order to induce reduction of a presumed sulfenic acid intermediate to the final thiol active metabolite) in 100 mM KPi buffer containing 100 mM NaF (200 μl final volume). The reaction rate at each substrate concentration was determined in triplicate. Reactions were preincubated at 37 °C/70 r.p.m. for 3 min before initiation with NADPH (1 mM final concentration) and were then incubated for 15 min before quenching with a 50% volume of an ice-cold solution of 80 nM prasugrel in acetonitrile. 2-Bromo-3′-methoxyacetophenone (30 μl from a 100 mM dimethyl sulfoxide stock solution) was added as a thiol derivatizing agent and the reactions were incubated for an additional 60 min at 37 °C/70 r.p.m. Protein was then removed by centrifugation and supernatants were analyzed by LC-MS/MS (Supplementary Methods).

Determination of CYP2C19 kinetic parameters. Kinetic parameters for (S)-mephenytoin 4′-hydroxylation by genotype-defined pooled HLMs were estimated by means of nonlinear least-squares analysis, using the MULTI program.[34] The affinity of (S)-mephenytoin for CYP2C19 (K_m) and the maximal velocity of CYP2C19-catalyzed (S)-mephenytoin 4′-hydroxylation

(V_{max}) were obtained by fitting the data to the Michaelis–Menten equation (Equation (1)):

$$V = \frac{V_{max}[S]}{K_m[S]} \quad (1)$$

where V is the initial metabolism rate of (S)-mephenytoin (pmol min^{-1} per mg protein), and [S] is the concentration of substrate, (S)-mephenytoin, in the incubation (μM).

Kinetic analyses of 2-oxo-clopidogrel and CAM formation data were performed on GraphPad Prism software, v. 5.03 (San Diego, CA, USA). The following two-enzyme kinetic model was fit to the biphasic data:[35]

$$V = \frac{V_{max(1)}[S] + V_{max(2)}[S]^2/K_{m(2)}}{K_{m(1)} + [S] + [S]^2/K_{m(2)}} \quad (2)$$

Eadie–Hofstee graphs for both steps of clopidogrel bioactivation were clearly nonlinear across all genotypes, and data comparisons performed in GraphPad Prism using the above two-enzyme model against standard Michaelis–Menten kinetics generated F-values well above 1 for all data sets ($9.5 < F < 120$), with P-values ≤ 0.0012, indicating the relative accuracy of the biphasic model.

Graphical presentation of the data included the best fitted regression line and data points denoting mean values and s.d. error bars from triplicate incubations at each substrate concentration. Tabular presentation of the data represents the mean values and s.d. error bars for parameter estimates determined from three replicate experiments.

Quantitation of total *P*450 protein content in HLMs

The contents of total *P*450 protein for pooled HLMs with defined homozygous diplotypes (*CYP2C19*1B/*1B*, **2A/*2A* and **17/*17*) were examined by reduced carbon monoxide difference spectral analysis measured on an Olis-modernized Aminco DW-2 spectrophotometer (Olis, Bogart, GA, USA). The detailed methods used are described in the Supplementary Methods.[36] All values were determined as means from duplicate experiments.

Quantitation of CYP2C19 and cytochrome *P*450 oxidoreductase protein content in HLMs

CYP2C19 and POR protein expression in individual or genotype-defined pooled HLM samples were determined by a surrogate peptide-based LC-MS/MS method. Synthetic surrogate peptides of CYP2C19 and POR for LC-MS/MS quantification were selected based on previously reported criteria (Supplementary Table 3).[37,38] The detailed methods used for protein quantitation are described in the Supplementary Methods.[39–41] The CYP2C19 and POR content of each individual microsomal preparation and pooled (based on diplotype) preparations were determined in triplicate. The protein expression data for pooled samples are reported as the mean and s.d. of values obtained from the three experimental determinations. When the measured result was below lower limit of quantification (LLOQ; or not detected), the LLOQ value was introduced as a substitute, although this has a slightly different meaning than $<$ LLOQ.

Statistical analysis

Multivariate linear regression analysis. A multivariate linear regression analysis of demographic and medical variables for the diplotyped liver donors was performed to elucidate major determinants of interindividual variability in CYP2C19 activity (Microsoft Office Excel 2010, Microsoft, Redmond, WA, USA). Full details are given in the Supplementary Methods section. A P-value of < 0.05 was considered to be statistically significant for all tests.

Other statistical analyses. The mephenytoin hydroxylation activity data for the full 347 liver data set exhibited a skewed distribution. Accordingly, the nonparametric Mann–Whitney test was performed for between-diplotype group comparisons in the study using individual HLMs. The two-sided unpaired Student's *t*-test, with unequal variances, was performed for *post hoc* between-diplotype group comparisons in the study using pooled HLMs. A correction for multiple comparisons was not applied. A linear trend test (one-way analysis of variance) was performed for the rank order analysis, and a P-value of < 0.05 was considered to be statistically significant.

RESULTS

Liver demographics

Characteristics of liver donors and the tissue itself are summarized in Table 1. A total of 347 liver samples from 200 male donors (mean age 37.7 years, range 0–81 years), 142 female donors (mean age 42.8 years, range 0–87 years) and 5 unknown were tested. The majority (96.3 %) of samples were of Caucasoid (White) origin. Of the 347 donors, 10 (2.88%) were not receiving medications at the time of death or tissue procurement, 154 (44.4%) were receiving one or more medications and 183 (52.7%) had no medication history reported. In addition, 119 donors (34.3%) had no disease at the time of death; 52 (15.0%) had liver disease including fatty liver, chronic hepatitis, fibrotic liver, hepatoma, acute injury and biliary atresia; 74 (21.3%) had any other diseases including cardiovascular disturbance, diabetes, cystic fibrosis and colorectal cancer; 102 (29.4%) were unknown regarding disease information. The cause of death was recorded by a forensic pathologist as: 99 donors (28.5%) had brain damage including cerebral vascular accident, head trauma, subarachnoid hemorrhage and intracerebral hemorrhage; 14 (4.03%) had suffered another accident including auto accident and gunshot; 226 (65.1%) were unknown regarding the cause of death.

CYP2C19 allele and diplotype frequencies

In the present study, 18 different variant alleles of *CYP2C19* were identified and they are listed in Table 2. Of these, *CYP2C19*1C* (80161A>G), **2A* (99C>T, 19154G>A, 80160C>T, 80161A>G) and **17* (−3402C>T, −806C>T, 99C>T, 80161A>G) consisted of synonymous or noncoding SNPs. Alleles containing nonsynonymous coding SNPs were *CYP2C19*1A*, **4B* (−3402C>T, −806C>T, 1A>G, 99C>T, 80161A>G), **6* (99C>T, 12748G>A, 80161A>G), **8* (12711T>C), **11* (99C>T, 12802G>A, 80161A>G), **13* (80161A>G, 87290C>T), *L14S* (37T>C), Q22R (65A>G), *G62R* (12368G>C), *R125H* (12727G>A), *R150C* (12801C>T), *G228E* (19155G>A), *D341H* (80191G>C) and *D360N* (80248G>A). These nsSNPs were classified into deleterious nsSNPs (*CYP2C19*4B*, **6*, **8*, *L14S*, *G62R*, *R125H*, *G228E*, *D341H* and *D360N* variant alleles) or benign nsSNPs (*CYP2C19*1A*, **11*, **13*, *Q22R* and *R150C* variant alleles) for the functional consequence (Supplementary Table 2). The other *CYP2C19*2* variant, **2B* (99C>T, 12460G>C, 19154G>A, 80160C>T, 80161A>G), was also detected in the set of human livers studied, but it was found at a low frequency ($< 5\%$), compared with *CYP2C19*2A*. The coding change (Glu92Asp) is predicted to be benign, but the phenotype is probably null because of the presence of the splice site variant (19154G>A) in the haplotype.

To characterize the association between gene diplotype and enzyme activity, we focused on the following alleles: *CYP2C19*1B*, **1C*, **2A* and **17*. From the panel of 347 human liver samples, the frequencies of the respective *CYP2C19*1B/*1B*, **1B/*1C*, **1C/*1C*, **1B/*2A*, **2A/*2A*, **1B/*17*, **17/*17*, **1C/*2A*, **1C/*17* and **2A/*17* diplotypes were 32.6% ($n = 113$), 0.576% ($n = 2$), 0% ($n = 0$), 12.1% ($n = 42$), 1.44% ($n = 5$), 19.0% ($n = 66$), 6.63% ($n = 23$), 0.288% ($n = 1$), 0% ($n = 0$) and 7.49% ($n = 26$), respectively (Table 1). The reference allele, *CYP2C19*1A*, was detected in only 24 livers. The frequencies of the liver groups with deleterious and benign nsSNPs were 2.59% ($n = 9$) and 17.3% ($n = 60$), respectively.

Impact of gene diplotype on CYP2C19-catalyzed metabolism of (S)-mephenytoin

CYP2C19 activity was measured using HLMs isolated from 347 genotyped liver samples and (S)-mephenytoin as a prototypical substrate. We saw no difference between the (S)-mephenytoin 4′-hydroxylase activity of HLMs from livers with the **1A/*1B* and **1B/*1B* diplotypes (data not shown). Because the frequency of *CYP2C19*1A* and **1C* alleles was remarkably low compared with that

Table 1. *CYP2C19* diplotype frequency and demographic characteristics of the liver cohort

CYP2C19 diplotype		**1B/*1B*	**1B/*2A*	**1B/*1C*	**2A/*2A*	**1B/*17*	**17/*17*	**1C/*2A*	**2A/*17*	*nsSNPs*[a]	*Total*
Number	(*n*)	113	42	2	5	66	23	1	26	69 (10)	347
Frequency	(%)	32.6	12.1	0.6	1.4	19	6.6	0.3	7.5	19.9 (2.88)	100
Age											
Average	(Years)	41	37.6	72.5	39	37.6	41.8	2	38.1	40.7 (37.4)	39.7
Max–min	(Range)	0–74	1–68	66–79	4–75	1–87	1–66	2	0–66	0–80 (2–66)	0–87
Unknown	(*n*)	8	0	0	2	1	3	0	5	3 (0)	22
Gender											
Male	(*n*)	68	27	2	3	34	13	0	13	40 (8)	200
Female	(*n*)	43	15	0	2	30	10	1	13	28 (2)	142
Unknown	(*n*)	2	0	0	0	2	0	0	0	1 (0)	5
Race											
White	(*n*)	108	41	1	4	65	20	1	25	67 (10)	332
Black	(*n*)	2	1	1	1	1	2	0	1	1 (0)	10
Hispanic	(*n*)	1	0	0	0	0	1	0	0	0 (0)	2
Unknown	(*n*)	2	0	0	0	0	0	0	0	1 (0)	3
Drug											
None	(*n*)	3	1	0	0	2	1	0	0	3 (1)	10
CYP inducer[b]	(*n*)	25	6	0	0	12	3	0	5	10 (4)	61
Noninducer	(*n*)	31	12	1	2	12	7	0	6	22 (2)	93
Unknown	(*n*)	54	23	1	3	40	12	1	15	34 (3)	183
Disease											
Normal	(*n*)	41	17	1	1	22	6	0	8	23 (6)	119
Liver	(*n*)	12	10	0	0	11	5	1	3	10 (0)	52
Others	(*n*)	29	6	1	1	17	3	0	2	15 (1)	74
Unknown	(*n*)	31	9	0	3	16	9	0	13	21 (3)	102
Death (COD)											
Brain	(*n*)	35	15	0	1	10	10	0	8	20 (3)	99
Others	(*n*)	6	1	1	0	4	0	0	0	2 (0)	14
Unknown	(*n*)	70	26	1	4	52	11	1	17	44 (7)	226
Living	(*n*)	2	0	0	0	0	2	0	1	3 (0)	8

Abbreviations: COD, cause of death; nsSNP, nonsynonymous single-nucleotide polymorphism. Deleterious nsSNP group includes *CYP2C19*4B*, **6*, **8*, *L14S*, *G62R*, *R125H*, *G228E*, *D341H* and *D360N* variant alleles (Supplementary Table 2). [a]The values in parenthesis are numbers of deleterious nsSNPs. [b]CYP inducer includes dexamethasone, prednisone, phenytoin and phenobarbital.

Table 2. *CYP2C19* variants identified in 347 human livers

Variants	*cDNA change*	*Gene change*	*Location*	*Amino acid change*	*rs (reference SNP) ID*
*CYP2C19*1A*	None	None	None	None	None
*CYP2C19*1B*	99C>T, **991A>G**	99C>T, **80161A>G**	Ex 7	I331V	rs3758581
*CYP2C19*1C*	**991A>G**	**80161A>G**	Ex 7	I331V	rs3758581
*CYP2C19*2A*	99C>T, **681G>A**, 990C>T, 991A>G	99C>T, **19154G>A**, 80160C>T, 80161A>G	Ex 5	I331V	rs4244285
*CYP2C19*2B*	99C>T, 276G>C, **681G>A**, 990C>T, 991A>G	99C>T, 12460G>C, **19154G>A**, 80160C>T, 80161A>G	Ex 2	Glu92Asp, I331V	rs17878459
*CYP2C19*4B*	**1A>G**, 99C>T, 991A>G	-3402C>T, -806C>T, **1A>G**, 99C>T, 80161A>G	Ex 1	Met1Val, I331V	rs28399504
*CYP2C19*6*	99C>T, **395G>A**, 991A>G	99C>T, **12748G>A**, 80161A>G	Ex 3	Arg132Gln, I331V	rs72552267
*CYP2C19*8*	358T>C	12711T>C	Ex 3	Trp120Arg	rs41291556
*CYP2C19*11*	99C>T, **449G>A**, 991A>G	99C>T, **12802G>A**, 80161A>G	Ex 3	Arg150His, I331V	rs58973490
*CYP2C19*13*	991A>G, **1228C>T**	80161A>G, **87290C>T**	Ex 8	I331V Arg410Cys	rs17879685
*CYP2C19*17*	99C>T, 991A>G	-3402C>T, **-806C>T**, 99C>T, 80161A>G	Promoter	I331V	rs12248560
L14S	37T>C	37T>C	Ex 1	Leu14Ser	None
Q22R	65A>G	65A>G	Ex 1	Gln22Arg	rs144928727
G62R	184G>C	12368G>C	Ex 2	Gly62Arg	None
R125H	373G>A	12727G>A	Ex 3	Arg125His	rs141774245
R150C	448C>T	12801C>T	Ex 3	Arg150Cys	rs142974781
G228E	682G>A	19155G>A	Ex 5	Gly228Glu	None
D341H	1021G>C	80191G>C	Ex 7	Asp341His	None
D360N	1078G>A	80248G>A	Ex 7	Asp360Asn	rs144036596

Abbreviations: cDNA, complementary DNA; SNP, single-nucleotide polymorphism. NT_030059.13 was used as the reference sequence. Nucleotide variations in bold are the major SNPs/alterations responsible for the phenotype of the corresponding allele.

of other alleles, only *CYP2C19*1B, *2A* and **17* alleles were used to test diplotype–activity association in subsequent analyses.

The Mann–Whitney test was performed for between-diplotype group comparisons (Table 3 and Supplementary Figure 1). In the group of HLMs with a *CYP2C19*2A/*2A* diplotype, the mean activity was only 5.14% of that found for the wild-type HLMs with a *CYP2C19*1B/*1B* diplotype. The mean activity for the *CYP2C19*1B/*2A* diplotype was 35.4% lower than that of the *CYP2C19*1B/*1B* diplotype, although the difference did not reach statistical significance. There was a trend for higher CYP2C19 activity in livers with a *CYP2C19*1B/*17* (1.05-fold) and **17/*17* (1.28-fold) diplotype, compared with the *CYP2C19*1B/*1B* diplotype, but again the head-to-head comparisons were not significantly different. In addition, the metabolic activity of the *CYP2C19*2A/*17* diplotype livers was on average 39.6% lower than that of the *CYP2C19*1B/*1B* diplotype livers, suggesting that there was not an equal offset of effects from the **2* and **17* alleles, but once again the difference was not significant. For the livers from donors carrying a nonsynonymous coding variant, the mean activity in the livers with deleterious nsSNPs was 14.9% lower than that in the livers with a *CYP2C19*1B/*1B* diplotype, although the difference did not reach statistical significance (Table 3). The metabolic activity of livers from donors carrying a benign nsSNP was not different from that of the *CYP2C19*1B/*1B* diplotype. Using a linear trend analysis, the *a priori* assigned rank order for enzyme activity of the common diplotypes (*CYP2C19*17/*17* > *1B/*17* > *1B/*1B* > *2A/*17* > *1B/*2A* > *2A/*2A*) was statistically significant ($P < 0.05$) (Figure 1).

LD between *CYP2C19*1B*, **2A* and **17* alleles

The LD between the common *CYP2C19* SNPs is visualized in Figure 2. The calculations show complete LD ($|D'| = 1$, LOD > 2) between *CYP2C19*2A* and **17*. Complete LD was also observed between *CYP2C19*1B* and **17*. However, although the analysis revealed $|D'| = 1$ between *CYP2C19*1B* and **2A* alleles, the LOD score < 2 indicates that the loci are not significantly linked. Even though *CYP2C19*2A* and **17* alleles are in complete LD, the correlation coefficient (r^2) between them was only 0.057. Low r^2 values were also observed between *CYP2C19*1B* and *CYP2C19*2A* and between *CYP2C19*1B* and **17* ($r^2 = 0.003$ and 0.017, respectively).

Table 3. Impact of *CYP2C19* diplotype on metabolism of (S)-mephenytoin in HLMs

CYP2C19 diplotypes	*Number* (n)	*Frequency (%)*	*(S)-Mephenytoin 4′-hydroxylation (pmol min^{-1} per mg protein)* Mean ± s.d.	*Statistical significance* P-value
**1B/*1B*	113	32.6	18.4 ± 25.1	1.00
**1B/*2A*	42	12.1	11.9 ± 14.3	0.182
**2A/*2A*	5	1.44	0.95 ± 1.2	0.00350[a]
**1B/*17*	66	19.0	19.2 ± 26.6	0.7236
**17/*17*	23	6.63	23.5 ± 39.2	0.812
**2A/*17*	26	7.49	11.1 ± 18.2	0.0552
Deleterious nsSNPs[b]	10	2.88	15.7 ± 29.3	0.352
Benign nsSNPs[c]	44	12.7	16.1 ± 24.1	0.210

Abbreviations: HLM, human liver microsome; nsSNP, nonsynonymous single-nucleotide polymorphism. [a]$P < 0.01$, significantly different from metabolic activity in HLMs with *CYP2C19*1B/*1B* diplotype. CYP2C19 metabolic activity data are shown as means ± s.d. [b]Deleterious nsSNP group includes *CYP2C19*4B*, **6*, **8*, *L14S*, *G62R*, *R125H*, *G228E*, *D341H* and *D360N* variant alleles (Supplementary Table 2). [c]Benign nsSNP group includes *CYP2C19*1A*, **11*, **13*, *Q22R* and *R150C* variant alleles (Supplementary Table 2). Statistical analyses were performed using the Mann–Whitney test (nonparametric test).

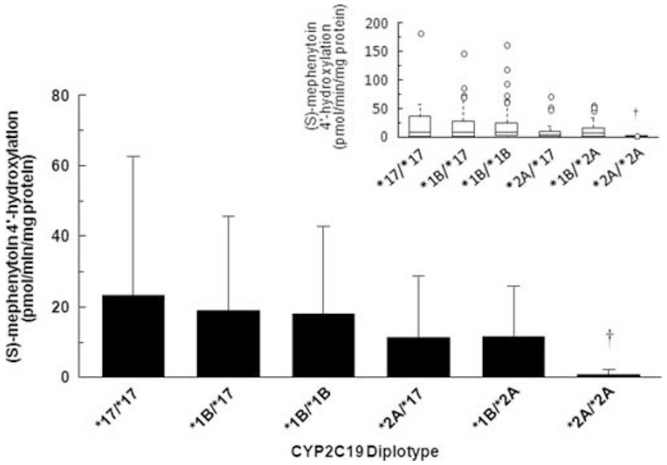

Figure 1. Association between *CYP2C19* diplotype and CYP2C19 metabolic activity. CYP2C19-catalyzed (S)-mephenytoin 4′-hydroxylation activity of 347 different human liver microsome (HLM) preparations was measured and segregated according to the observed *CYP2C19* diplotypes. Data (closed bars) are presented as mean ± s.d. The insert is a box-and-whisker plot (Tukey's box plot). The box represents the 25th and 75th percentiles enclosing a median bar, and the whiskers represent the highest and lowest values that are not outliers or extreme values. Outliers (values that are more than 1.5 times the interquartile range) are individually represented by open circles beyond the whiskers. A linear trend test (one-way analysis of variance (ANOVA)) was performed for the rank order and was found to be significant ($P < 0.05$). A two-sided, unpaired Student's *t*-test was employed for *post hoc*, pairwise comparisons; †$P < 0.05$, significantly different from metabolic activity in HLM with *CYP2C19*1B/*1B* diplotype.

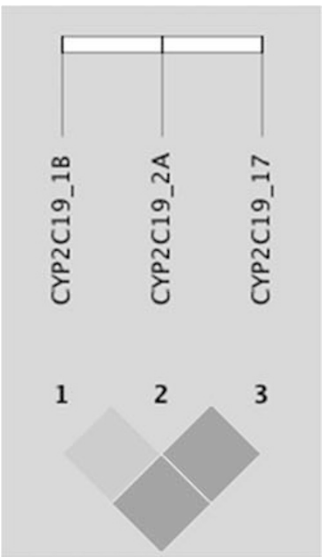

Figure 2. Linkage disequilibrium (LD) map for the common *CYP2C19* allelic variants. An LD map of the *CYP2C19*1B*, **2A* and **17* alleles was created using Haploview 4.2. The dark gray (the red in a full colour version) squares show complete LD with statistical significance ($|D'| = 1$, LOD > 2), and the light gray (the blue in a full colour version) square shows complete LD, but lacking statistical significance ($|D'| = 1$, LOD < 2). LOD, logarithm of odds. A full colour version of this figure is available at the *The Pharmacogenomics Journal* journal online.

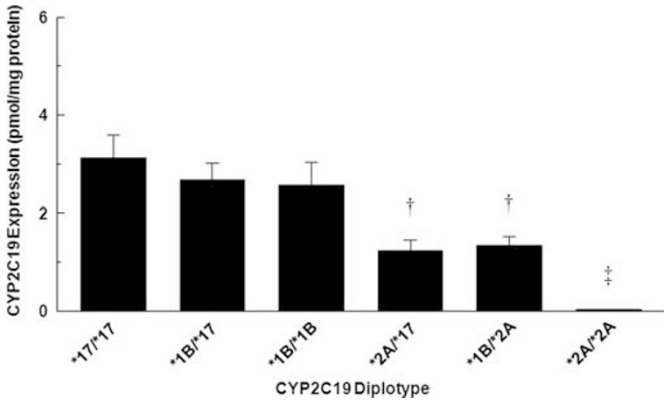

Figure 3. Association between *CYP2C19* diplotype and CYP2C19 protein content in genotype-defined pooled human liver microsomes (HLMs). The absolute abundance of CYP2C19 protein was quantified by surrogate peptide-based liquid chromatography–tandem mass spectrometry (LC-MS/MS) analysis. Data (closed bars) are presented as means ± s.d. ($n = 3$ replicate determinations). A linear trend test (one-way analysis of variance (ANOVA)) was performed for the rank order and was found to be statistically significant ($P < 0.0001$). A two-sided, unpaired *t*-test was employed for *post hoc*, pairwise comparisons; $^{\dagger}P < 0.05$, significantly different from CYP2C19 protein content in HLMs with *CYP2C19*1B/*1B* diplotype. $^{\ddagger}P < 0.01$, significantly different from CYP2C19 protein content in HLMs with *CYP2C19*1B/*1B* diplotype.

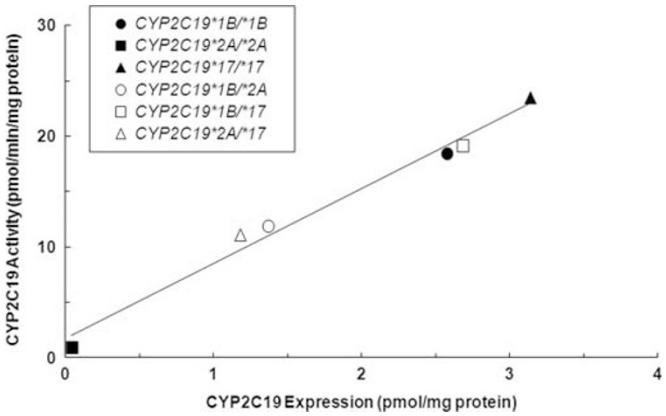

Figure 4. Correlation between CYP2C19 metabolic activity and protein content in genotype-defined pooled human liver microsomes (HLMs). CYP2C19-catalyzed (S)-mephenytoin 4′-hydroxylation activity and CYP2C19 protein content for genotype-defined pooled HLMs (*CYP2C19*1B/*1B* (filled circles), *CYP2C19*2A/*2A* (filled squares), *CYP2C19*17/*17* (filled triangles), *CYP2C19*1B/*2A* (open circles), *CYP2C19*1B/*17* (open squares) and *CYP2C19*2A/*17* (open triangles) diplotypes) were measured. Individual data points represent the mean of triplicate protein and activity determinations. Approximately 98% of the variability in CYP2C19 activity in the different diplotype pools could be explained by CYP2C19 protein variability ($r^2 = 0.984$).

Correlation between CYP2C19 metabolic activity and protein expression

The CYP2C19 protein content for pooled HLMs from donors with a defined CYP2C19 diplotype is presented in Figure 3. As expected, in the group of HLMs with a *CYP2C19*2A/*2A* diplotype, the mean CYP2C19 protein level was negligible compared with that found for the wild-type HLMs with a *CYP2C19*1B/*1B* diplotype. The mean protein level for the *CYP2C19*1B/*2A* diplotype was 46.9% lower than that of the *CYP2C19*1B/*1B* diplotype ($P < 0.05$). There was a trend for a higher CYP2C19 protein level in livers with a *CYP2C19*17/*17* (1.22-fold) diplotype, compared with the *CYP2C19*1B/*1B* diplotype, although the differences did not reach statistical significance. The protein level of the *CYP2C19*2A/*17* diplotype livers was significantly lower than that of the *CYP2C19*1B/*1B* diplotype livers. Using a linear trend analysis, the rank order of enzyme protein level for the common diplotypes (*CYP2C19*17/*17* > **1B/*17* > **1B/*1B* > **2A/*17* > **1B/*2A* > **2A/*2A*) was significant ($P < 0.0001$). A strong correlation was observed between CYP2C19 activity and protein content in these six genotype-defined HLMs groups ($r^2 = 0.984$; Figure 4).

POR content in HLMs

The mean POR protein contents for HLMs from donors with *CYP2C19*1B/*1B*, **1B/*2A*, **2A/*2A*, **1B/*17*, **17/*17* and **2A/*17* diplotypes were 22.5 ± 12.6, 31.6 ± 16.4, 24.9 ± 17.2, 21.8 ± 11.4, 27.7 ± 11.9 and 22.0 ± 9.5 pmol per mg protein, respectively. There was no significant difference in the mean POR protein content of the different diplotype groups. A linear trend analysis also showed no significant rank order correlation between CYP2C19 diplotype and POR level, indicating that POR variability could be an independent determinant of CYP2C19-catalyzed drug metabolism. Similar results for the POR protein contents were obtained from pooled HLMs (Supplementary Figure 2).

Multivariate linear regression analysis for factors affecting interindividual variability of CYP2C19-catalyzed (S)-mephenytoin metabolism

The results of the multivariate linear regression analysis, with missing values imputed, for the identification of predictors that affect interindividual variability in CYP2C19-catalyzed (S)-mephenytoin 4′-hydroxylation can be found in Table 4. The coefficient of determination (R^2 value) for the multivariate linear regression was 0.129, indicating that ~13% of interindividual variability of CYP2C19 activity is explained by the predictors in the model. The *CYP2C19*2A* and POR are significant predictors of CYP2C19 activity, with *P*-values of 0.000719 and 8.00×10^{-6}, respectively. The effect size (β-value) of the *CYP2C19*2A* allele was −10.5, indicating that each copy of the **2A* allele inherited by an individual results in an average decrease of −10.5 pmol min^{-1} per mg protein in CYP2C19 activity. All other covariates were not significant, including *CYP2C19*17*, that had a *P*-value of 0.585. We also conducted a multivariate regression analysis without imputing missing data and including only *CYP2C19*2A*, *CYP2C19*17* and POR as covariates (Supplementary Table 4). Here the results were similar, where *CYP2C19*2A* and POR are significant predictors of CYP2C19 activity in the reduced model, with *P*-values of 0.00106 and 3.61×10^{-6}, respectively. Again, *CYP2C19*17* was not a significant factor in the reduced model. The R^2 value for the multivariate linear regression was 0.103.

Kinetic analysis of CYP2C19-catalyzed (S)-mephenytoin metabolism by pooled HLMs from donors with homozygous *CYP2C19* diplotypes

The mechanism for the effect of *CYP2C19* diplotype on enzyme activity was examined, in part, by determining the enzyme concentration dependence of the CYP2C19-catalyzed 4′-hydroxylation of (S)-mephenytoin in pooled HLMs with defined homozygous diplotypes (*CYP2C19*1B/*1B*, **2A/*2A* and **17/*17*) (Figure 5). The average expression levels of *P*450, CYP2C19 and POR proteins in these pooled HLMs are shown in Figure 6. The

Table 4. Multivariate linear regression analysis for factors affecting interindividual variability of CYP2C19-catalyzed (S)-mephenytoin metabolism

Dependent	*Independent*	*β (coefficient)*	*s.e.*	*t-Stat*	P-*value*
CYP2C19 activity	Intercept	25.8	11	2.34	0.0198
	*CYP2C19*2A* allele	−10.5	3.06	−3.42	0.0007
	*CYP2C19*17* allele	1.24	2.27	0.546	0.585
	Cytochrome *P*450 oxidoreductase	0.513	0.113	4.56	8.00×10^{-6}
	Gender	−4.48	2.95	−1.52	0.129
	Race	−11.8	7.84	−1.5	0.134
	Medication (CYP inducer)	−8.16	4.42	−1.84	0.0662
	Liver disease	−3.52	4.23	−0.834	0.405
	Brain damage	−1.36	6.49	−0.21	0.834

We considered CYP2C19 metabolic activity as the response in the multivariate regression analysis with the following covariates: *CYP2C19*2A* allele (no copy = 0, one copy = 1, two copies = 2), *CYP2C19*17* allele (no copy = 0, one copy = 1, two copies = 2), *P*450 oxidoreductase (POR), gender (female = 0, male = 1), race (non-white = 0, white = 1), medication (no CYP inducer = 0, CYP inducer = 1), liver disease (absent = 0, present = 1) and brain damage (no = 0, yes = 1). β is the standard regression coefficient; *t*-Stat is *t*-statistic. The coefficient of determination (R^2 value) for the multivariate linear regression was 0.129.

CYP2C19 activities were normalized to HLM protein (Figure 5a), total *P*450 (Figure 5b) and CYP2C19 protein levels (Figure 5c).

The formation of 4′-hydroxy (S)-mephenytoin by pooled HLMs from donors with *CYP2C19*1B/*1B* and **17/*17* diplotypes was saturable, but not so for the *CYP2C19*2A/*2A* diplotype. Parameters obtained from the kinetic analysis are summarized in Table 5. Compared with HLMs from donors with a *CYP2C19*1B/*1B* diplotype, HLMs from donors with a *CYP2C19*17/*17* diplotype exhibited a significantly increased V_{max} value for the reaction, when normalized for total HLM protein content, and no significant change in K_m value. Overall, the metabolic efficiency, evaluated as V_{max}/K_m value, was significantly increased by 20.1%. When the activities were normalized to either the total *P*450 or CYP2C19 protein levels, to assess the intrinsic function of CYP2C19.1B and other variant CYP2C19 enzymes, the V_{max}/K_m values were found to be comparable for *CYP2C19*1B/*1B* and **17/*17* diplotypes. The V_{max} value on the basis of CYP2C19 protein level was also comparable for *CYP2C19*1B/*1B* and **17/*17* diplotypes, whereas the V_{max} values on the basis of *P*450 protein level was significantly lower in *CYP2C19*17/*17* diplotype than in the *CYP2C19*1B/*1B* diplotype. In the case of HLMs with a *CYP2C19*2A/*2A* diplotype, nonsaturable product formation kinetics was observed. V_{max}/K_m values derived from the linear curves revealed a significant decrease compared with HLMs with a *CYP2C19*1B/*1B* diplotype, indicative of complete loss of CYP2C19 activity, with low residual activity represented by another nonsaturable enzyme (Table 5). Similarly, a significant decrease in the V_{max}/K_m values were observed even though the activities were normalized to *P*450 protein levels. However, as shown in Figure 6, CYP2C19 protein level was negligible in HLMs with *CYP2C19*2A/*2A* diplotype. Therefore, normalization of the activity to the CYP2C19 protein gives an exaggerated rate of metabolism, when compared with the other diplotypes, where CYP2C19 is expressed.

Kinetic analysis of CYP2C19-catalyzed clopidogrel and 2-Oxo-clopidogrel metabolism by pooled HLMs from donors with homozygous CYP2C19 diplotypes

To explore the impact of the *CYP2C19* diplotype on the metabolism of a clinically relevant substrate for the encoded enzyme, kinetic analysis of CYP2C19-catalyzed clopidogrel and 2-oxo-clopidogrel metabolism was undertaken in pooled HLMs with defined homozygous diplotypes (Figure 7). Formation of the active thiol metabolite of clopidogrel (CAM) is thought to proceed through two consecutive *P*450-dependent oxidation steps: clopidogrel to 2-oxo-clopidogrel and then 2-oxo-clopidogrel to a sulfenic acid intermediate that undergoes subsequent glutathione-mediated reduction to give CAM. Therefore, the kinetic characteristics of each step were studied separately with pooled HLMs with defined homozygous diplotypes, as described above for the marker substrate, (S)-mephenytoin. In contrast to (S)-mephenytoin, both clopidogrel bioactivation steps exhibited multiphasic kinetics that could be described adequately by a two-enzyme model. Because of the significant difference in total *P*450 content between the different CYP2C19 diplotype pools and the multienzyme nature of the clopidogrel bioactivation steps, for our primary analysis, we elected to compare catalytic activities that were normalized for total *P*450 (Figures 7c and d) rather than total HLM protein (Figures 7a and b), although data normalized for total HLM protein and CYP2C19 protein levels (Figures 7e and f) are presented for completeness. Regardless of the pathway studied, all extracted kinetic parameters for the pooled HLMs with *CYP2C19*1B/*1B* and *CYP2C19*17/*17* diplotypes were of similar magnitude, when normalized for total *P*450 content (Table 6). In contrast, the HLMs from donors with a *CYP2C19*2A/*2A* diplotype exhibited lower intrinsic clearances (V_{max}/K_m) to both 2-oxo-clopidogrel and CAM for the high- and low-affinity enzymatic components. For either reaction, it is likely that only the high-affinity enzymes are relevant to the *in vivo* metabolism of the drug, and hence relative enzymatic efficiencies are discussed below only in terms of this component.

The high-affinity intrinsic clearance (V_{max}/K_m) to 2-oxo-clopidogrel was reduced by 52% in the pooled HLMs with the *CYP2C19*2A/*2A* diplotype relative to *CYP2C19*1B/*1B* diplotype, and by 84% for the second bioactivation step to CAM. For CAM formation, the K_m value increased fivefold (to ~5 μM) in the pooled HLMs with the *CYP2C19*2A/*2A* diplotype, reflective of the absence of CYP2C19 enzyme, and likely represents catalysis by other slightly lower affinity *P*450s such as CYP3A4 and CYP2C9.[42] Interestingly, no significant change in K_m value was observed for the first bioactivation step in the pooled HLMs with the *CYP2C19*2A/*2A* diplotype, but again this is in agreement with the microsomal kinetic studies of Kazui *et al.*[42] who observed that CYP1A2 and CYP2B6 possessed similarly low K_m values to CYP2C19 for this reaction. Normalization of the activity to the CYP2C19 protein level exhibited more variable V_{max} and V_{max}/K_m values compared with those on the basis of *P*450 protein level (Table 6). These findings support the consideration described above that 2-oxo-clopidogrel and CAM formations are catalyzed by multiple *P*450 enzymes with different affinity for each reaction.

DISCUSSION

Of the 19 *CYP2C19* alleles observed, 3 are thought to confer wild-type activity (*CYP2C19*1A*, *CYP2C19*1B* and *CYP2C19*1C*). The 80161G (331V) variant, representing the *CYP2C19*1B* allele, was

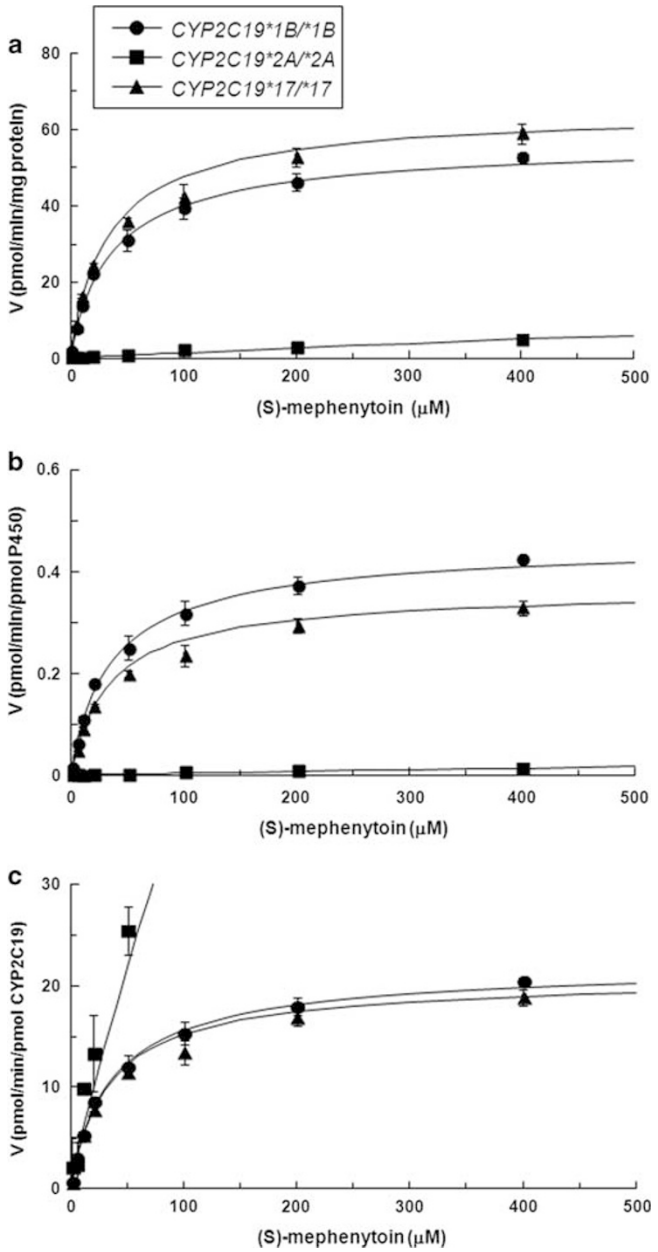

Figure 5. Kinetic analysis of CYP2C19-catalyzed (S)-mephenytoin metabolism by pooled human liver microsomes (HLMs) from donors with homozygous *CYP2C19* diplotypes. (S)-Mephenytoin 4′-hydroxylation by HLMs with homozymous diplotype (*CYP2C19*1B/*1B* (filled circles), *CYP2C19*2A/*2A* (filled squares) and *CYP2C19*17/*17* (filled triangles)) was measured at substrate concentrations between 1 and 400 μM. (**a**) Results normalized for HLM protein content. (**b**) Results normalized for functional *P*450 content. (**c**) Results normalized for CYP2C19 protein content. Each data point is the mean velocity of the reaction ± s.d. (from three replicate determinations).

more frequently observed in our study population when compared with the 80161A (331I) allele, designated *CYP2C19*1A*.[43] Accordingly, the *CYP2C19*1A/*1B* and **1B/*1B* diplotypes were also more frequently encountered in our sample set (Supplementary Table 5). Based on prevalence and catalytic activity, we used *CYP2C19*1B/*1B* microsomes as the reference for all subsequent diplotype comparisons.

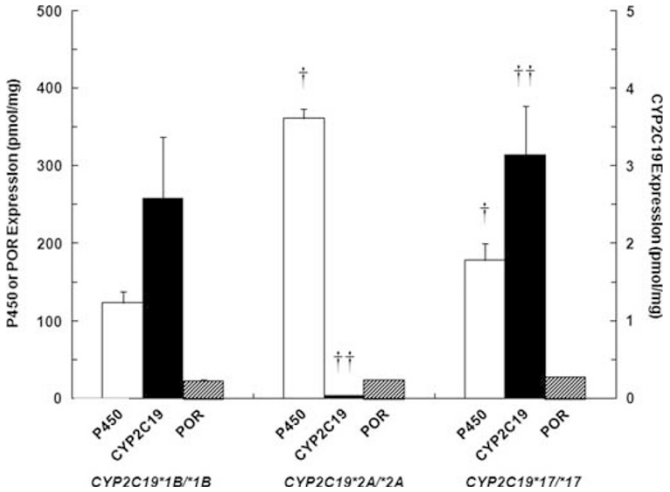

Figure 6. Total *P*450 protein, CYP2C19 protein and cytochrome *P*450 oxidoreductase (POR) protein expression levels in pooled human liver microsomes (HLMs) from donors with homozygous *CYP2C19* diplotypes. Total *P*450 protein expression level (open bars) in HLMs with homozygous diplotype (*CYP2C19*1B/*1B*, *CYP2C19*2A/*2A* and *CYP2C19*17/*17*) was measured by reduced 2-oxo-clopidogrel (CO) difference spectral analysis. CYP2C19 protein (closed bars) and POR protein (hatched bars) expression levels in HLMs with homozygous diplotype were measured by liquid chromatography–tandem mass spectrometry (LC-MS/MS) analysis. Data are shown as means ± s.d. from three replicate determinations. A two-sided, unpaired *t*-test was employed for *post hoc*, pairwise comparisons; $^{\dagger}P < 0.05$, significantly different from total *P*450 protein expression in wild-type HLMs with *CYP2C19*1B/*1B* diplotype. $^{\dagger\dagger}P < 0.05$, significantly different from CYP2C19 protein expression in wild-type HLMs with *CYP2C19*1B/*1B* diplotype.

The *CYP2C19*17* and **2A* variants accounted for the remainder of the common diplotypes, with frequencies ranging from 7.5 to 33%. Given that 96.3% of the liver donors in this study were identified racially as White, the diplotype frequencies were as expected and consistent with a previous report showing that *CYP2C19*17* allele is more frequently observed compared with the *CYP2C19*2* allele in Whites.[10]

Three of the nine possible diplotype combinations from the **1B*, **17* and **2A* alleles, **1B*2A/*17*17*, **2A*2A/*1B*17* and **2A*2A/*17*17*, were not observed in our samples, implying the absence of the **2A/*17* haplotype (Table 1). Further analysis revealed that *CYP2C19*2A* and **17* alleles were in complete LD ($|D'| = 1$, LOD > 2) (Figure 2). Complete LD was also observed between *CYP2C19*1B* and **17* alleles. However, despite the fact that the *CYP2C19*17* (−806T) variant appeared to be always found on the haplotype lacking the *CYP2C19*2A* (19154A) variant, the r^2 value between the two loci was low ($r^2 = 0.057$). This is likely because the reference allele at the *CYP2C19*2A* locus is much more common than *CYP2C19*17* and hence is also seen with the reference allele at the *CYP2C19*17* locus. This finding is similar to that reported in recent studies, where it was also concluded that individuals heterozygous or homozygous for the *CYP2C19*17* allele are less likely to carry the *CYP2C19*2* allele, whereas those who are wild type at the *CYP2C19*17* locus are more likely to carry the *CYP2C19*2* allele.[26,44]

A linear trend analysis revealed that the rank order for CYP2C19 activity (**17/*17* > **1B/*17* > **1B/*1B* > **2A/*17* > **1B/*2A* > **2A/*2A*) was statistically significant. This is in good agreement with a clinical report describing an association between *CYP2C19* polymorphisms and single-dose pharmacokinetics of oral pantoprazole in healthy volunteers. The under the concentration-time

Table 5. Kinetic parameters (K_m and V_{max}) for CYP2C19-catalyzed (S)-mephenytoin metabolism in pooled human liver microsomes (HLMs) from donors with a homozygous *CYP2C19* diplotype

		V_{max}			V_{max}/K_m		
Pooled HLM with CYP2C19 diplotypes	*K_m (μM)*	*Protein[a] (pmol min^{-1} per mg protein)*	*P450[b] (pmol min^{-1} per pmol P450)*	*CYP2C19[c] (pmol min^{-1} per pmol CYP2C19)*	*Protein[a] (μl min^{-1} per mg protein)*	*P450[b] (μl min^{-1} per pmol P450)*	*CYP2C19[c] (μl min^{-1} per pmol CYP2C19)*
**1B/*1B*	38.4 ± 6.7	57.1 ± 3.3	0.461 ± 0.027	22.2 ± 1.3	1.51 ± 0.20	0.0122 ± 0.0016	0.586 ± 0.077
**2A/*2A*	—	—	—	—	0.0114 ± 0.0058‡	0.0000317 ± 0.0000162‡	—
**17/*17*	34.7 ± 2.7	65.5 ± 0.5†	0.366 ± 0.003‡	20.9 ± 0.2	1.89 ± 0.13†	0.0106 ± 0.0007	0.604 ± 0.043

Kinetic parameters were obtained from the data presented in Figure 5. Total *P*450 protein and CYP2C19 protein level data are derived from Figure 6. †$P < 0.05$, significantly different from kinetic parameter in HLMs with *CYP2C19*1B/*1B* diplotype. ‡$P < 0.01$, significantly different from kinetic parameter in HLMs with *CYP2C19*1B/*1B* diplotype. Data are shown as means ± s.d. from three experiments. [a]Parameters normalized for HLM protein content. [b]Parameters normalized for total *P*450 content. [c]Parameters normalized for CYP2C19 protein content. Because CYP2C19 protein level is negligible in HLMs with *CYP2C19*2A/*2A* diplotype, as shown in Figure 6, normalization of the activity to the CYP2C19 protein gives an exaggerated rate of metabolism when compared with the other diplotypes. To avoid confusion, the CYP2C19 normalized rate is not included.

curve of pantoprazole was lowest in subjects with a reported *CYP2C19*17/*17* diplotype, followed by *CYP2C19*1/*17*, **1/*1*, **2/*17* and **1/*2* diplotypes, and highest in subjects with the **2/*2* diplotype.[25] Individuals with the *CYP2C19*17* variant are also reported to exhibit enhanced metabolic clearance of several other drugs, including omeprazole, amitriptyline, voriconazole and escitalopam.[9,20–25] Of the diplotypes that were observed in our study, the mean activity was greatly decreased in HLMs with the *CYP2C19*2A/*2A* diplotype compared with HLMs with a *CYP2C19*1B/*1B* diplotype. Moreover, HLMs from *CYP2C19*2A/*2A* diplotype livers exhibited nonsaturable metabolic kinetics, indicative of a complete loss of CYP2C19 expression. Indeed, CYP2C19 protein was negligible in all livers with a homozygous *CYP2C19*2A/*2A* diplotype.

In contrast, our findings demonstrated that inheritance of the *CYP2C19*17* allele is associated with increased hepatic CYP2C19 protein content, as indicated by an increased V_{max} value for (S)-mephenytoin 4′-hydroxylation and CYP2C19 protein content for pooled livers homozygous for the **17* allele and lacking the **2A* allele in comparison with those homozygous for *CYP2C19*1B*. This same trend was observed when liver activity was examined individually, although the considerable within-diplotype group variability reduced the power of the analysis; only a trend test for the *a priori* rank order assignment was significant. These results support the hypothesis that the SNP described by the **17* locus enhances *CYP2C19* transcription and protein synthesis, although the effect size is modest. This conclusion is also bolstered by the fact that the K_m value for (S)-mephenytoin 4′-hydroxylation in the *CYP2C19*17/*17* livers was not altered in comparison with that for the *CYP2C19*1B/*1B* diplotype; the structure of the protein generated from each allele would be unchanged. Of note, the K_m value for (S)-mephenytoin 4′-hydroxylation associated with the *CYP2C19*1B/*1B* diplotype was comparable to a previously reported value reported for microsomes isolated from yeast cells expressing *CYP2C19* alleles.[45]

The Clinical Pharmacogenetics Implementation Consortium has classified *CYP2C19*17* carriers as ultrarapid metabolizers in the context of clopidogrel metabolism to an active thiol metabolite (CAM).[46] However, we were unable to demonstrate a significant difference in the formation of 2-oxo-clopidogrel from clopidogrel or CAM from 2-oxo-clopidogrel by HLMs from donors with a *CYP2C19*17/*17* diplotype compared with the *CYP2C19*1B/*1B* diplotype. This appears to be a consequence of the fact that CYP2C19 is only one of multiple enzymes catalyzing each reaction and, thus, there is reduced penetrance from a relatively weak enzyme activity modifier (**17*). Our finding is consistent with the recent observations of Shuldiner and colleagues,[26] who saw no significant change in CAM or adenosine diphosphate-stimulated platelet aggregation in individuals with *CYP2C19*1/*1*, **1/*17* and **17/*17* diplotypes. Furthermore, *CYP2C19*1/*2* and **2/*17* diplotypes also yielded similar results. In contrast, HLMs from donors with a *CYP2C19*2A/*2A* diplotype exhibited lower activity for the conversion of both clopidogrel to 2-oxo-clopidogrel and 2-oxo-clopidogrel to CAM, although the relative effect size of the variant SNP at the **2* locus on the high-affinity (low K_m) component of the clopidogrel and 2-oxo-clopidogrel oxidation reaction was smaller than that observed for (S)-mephenytoin 4′-hydroxylation. This matches with what has been observed *in vivo* with regard to clopidogrel metabolism and that of more selective CYP2C19 substrates.[11,26,47,48]

There were a number of *CYP2C19* nsSNPs detected in our panel of livers (~20% of the total), and hence it is possible that they contributed to interindividual variability of CYP2C19-catalyzed drug metabolism (Table 1). Although there was a trend for lower CYP2C19 activity in livers with a deleterious nsSNPs as compared with the *CYP2C19*1B/*1B* diplotype, the head-to-head differences were not significant. Individually, the benign nsSNPs were too infrequent for comparison with the observed metabolic activities, particularly given the considerable within-group variability of the *CYP2C19*1B/*1B* diplotype. Further studies with a larger sample size would be needed to dissect out any impact of nsSNPs on CYP2C19 activity.

It is also possible that extreme variability in CYP2C19 activity and protein content detected *in vitro* is an artifact of conditions present following brain death and organ procurement. A number of the liver donors were receiving medications with the potential to modulate metabolizing enzyme activity up and down, such as dexamethasone, ketoprofen, prednisone, phenytoin, cimetidine, amiodarone and phenobarbital.[49–53] Moreover, 15.0% of liver donors were patients with evidence of liver disease and/or had liver surgery, including fatty liver, chronic hepatitis, fibrotic liver, cirrhosis, hepatoma, acute injury, biliary atresia and cholangiocarcinoma. It was reported that CYP2C19-mediated metabolism of (S)-mephenytoin is quite sensitive to the presence of liver disease (CYP2C19 activity is reduced at an early stage of disease).[54] Therefore, the extreme distribution of our measured activity data may be explained in part by the presence of liver disease. In addition, 28.5% of liver donors had brain damage, including cerebral vascular accident, head trauma, subarachnoid hemorrhage and intracerebral hemorrhage, as the cause of death.

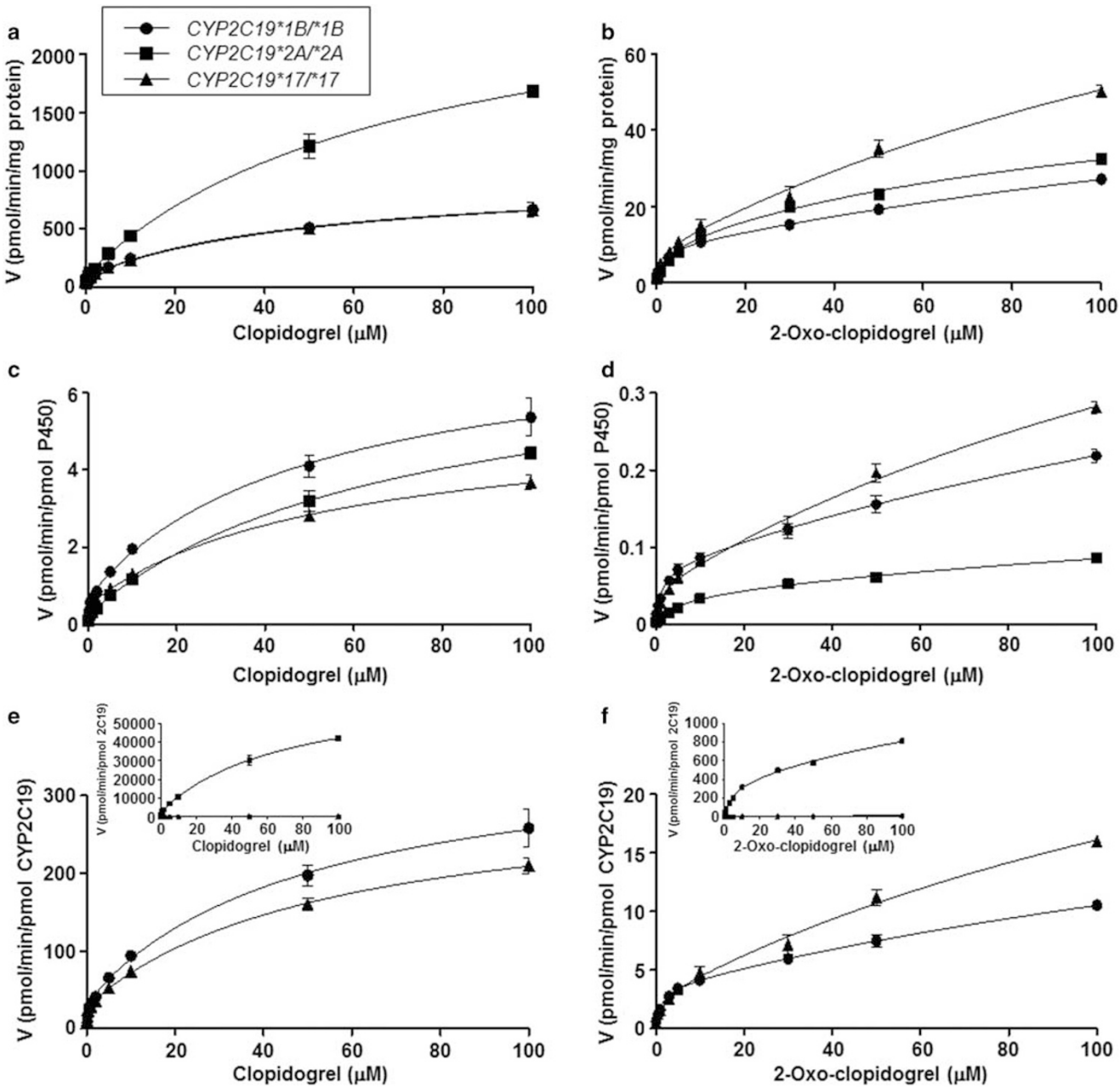

Figure 7. Kinetic analysis of CYP2C19-catalyzed clopidogrel and 2-oxo-clopidogrel (OC) metabolism by pooled human liver microsomes (HLMs) from donors with homozygous *CYP2C19* diplotypes. Kinetics of formation of (**a**, **c** and **e**) OC from clopidogrel and (**b**, **d** and **f**) clopidogrel active metabolite (CAM) from OC was studied separately by HLMs with a homozygous diplotype (*CYP2C19*1B/*1B* (filled circles), *CYP2C19*2A/*2A* (filled squares) and *CYP2C19*17/*17* (filled triangles)). (**a** and **b**) Results normalized for HLM protein content. (**c** and **d**) Results normalized for functional *P*450 content. (**e** and **f**) Results normalized for CYP2C19 protein content. Each data point is the mean velocity of the reaction ± s.d. from three replicate determinations.

Because an increase in inflammatory cytokines have been noted in both the serum and cerebrospinal fluid of patients with traumatic brain injury, it may be important to consider the influence of the endogenous cytokines on expression of CYP enzymes in donor organs.[55] Indeed, it was previously shown that various cytokines, such as interleukin-1β, interleukin-4, interleukin-6, tumor necrosis factor and interferon, act directly on human hepatocytes to affect expression of major *P*450 genes (CYP1A2, CYP2C, CYP2E1 and CYP3A) and associated enzymatic activity.[56] Similarly, altered hepatic CYP expression and antioxidant activity have been reported following endotoxin (lipopolysaccharide) or pro-inflammatory cytokine administration.[57] Although pre-existing liver disease and induced inflammation remain possible sources of interindividual variability in hepatic CYP2C19 activity, results from our multivariate analysis indicated no significant effect, possibly because of incomplete medical information in the donor population. Another possible explanation for a substantial fraction of interliver differences in CYP2C19 activity is the effect of gender on CYP2C19 activity and protein content. Indeed, recent report showed sex differences in the expression of hepatic drug-metabolizing enzymes.[58,59] Interestingly, growth hormone exerts sex-dependent effects on the liver in many species, with many

Table 6. Kinetic parameters (K_m and V_{max}) for both *P*450-dependent clopidogrel bioactivation steps in pooled human liver microsomes (HLMs) from donors with a homozygous *CYP2C19* diplotype

			V_{max}[a]			V_{max}/K_m		
Bioactivation steps	*Pooled HLM with CYP2C19 diplotypes*	K_m[a] (μM)	*Protein*[b] *(pmol min^{-1} per mg protein)*	*P450*[c] *(pmol min^{-1} per pmol P450)*	*CYP2C19*[d] *(pmol min^{-1} per pmol CYP2C19)*	*Protein*[b] *(μl min^{-1} per mg protein)*	*P450*[c] *(μl min^{-1} per pmol P450)*	*CYP2C19*[d] *(μl min^{-1} per pmol CYP2C19)*
Clop to OC	**1B/*1B*	0.300 ± 0.220	99.7 ± 24.0	0.804 ± 0.193	38.7 ± 9.3	332 ± 323	2.69 ± 2.62	129 ± 126
	**2A/*2A*	0.240 ± 0.180	115 ± 29.5‡	0.302 ± 0.078	2869 ± 738	479 ± 480	1.27 ± 1.28	13 700 ± 13 800
	**17/*17*	0.210 ± 0.080	96.6 ± 11.6	0.540 ± 0.065†	30.8 ± 3.7	460 ± 230	2.57 ± 1.29	147 ± 74
OC to CAM	**1B/*1B*	1.16 ± 0.27	9.39 ± 0.84	0.0760 ± 0.0070	3.64 ± 0.33	8.09 ± 2.61	0.0660 ± 0.0210	3.14 ± 1.01
	**2A/*2A*	4.71 ± 1.47	11.1 ± 2.16‡	0.0410 ± 0.0080‡	381 ± 76	2.36 ± 1.20	0.00900 ± 0.00400†	80.9 ± 41.1
	**17/*17*	0.71 ± 0.38	8.81 ± 1.63	0.0490 ± 0.0090‡	2.81 ± 0.52	12.4 ± 8.9	0.0690 ± 0.0490	3.96 ± 2.84

Abbreviations: CAM, clopidogrel active metabolite; Clop, clopidogrel; OC, 2-oxo-clopidogrel. Kinetic parameters were obtained from the data presented in Figure 7. Total *P*450 protein and CYP2C19 protein level data are derived from Figure 6. Error values, determined by GraphPad Prism software, are given in s.e.m. †$P < 0.05$, significantly different from kinetic parameter in HLMs with *CYP2C19*1B/*1B* diplotype. ‡$P < 0.01$, significantly different from kinetic parameter in HLM with *CYP2C19*1B/*1B* diplotype. [a]A biphasic curve provided the best fit to the data. the listed K_m and V_{max} values were determined for the high-affinity binding sites (low-affinity K_m values were estimated at 50 μM or above for both oxidation steps, across all three genotypes, and were thus considered physiologically irrelevant). [b]Parameters normalized for HLM protein content. [c]Parameters normalized for total *P*450 content. [d]Parameters normalized for CYP2C19 protein content.

hepatic genes, most notably genes coding for *P*450 enzymes, being transcribed in a sex-dependent manner. In the present study, we also examined CYP2C19 activity and protein content as a function of gender but found no significant difference (Table 1). As described in Table 4, the results of our multivariate linear regression analysis revealed that gender, as well as race, medication, liver disease and brain damage, was not a significant contributor to variability in the CYP2C19 activity in HLMs. This apparent inconsistency between our results and that of other investigators could be the result of inadequate power in our study. Finally, other uncontrolled aspects of the cellular environment, such as the impact of diet and disease, could contribute to the variability observed, possibly by epigenetic mechanisms.

We also explored the possibility that the availability of POR affected CYP2C19 activity, given its essential role in the catalytic process as an electron donor and prior observations that genetic variation in the POR gene can modulate *P*450 enzyme activity. The results of our multivariate linear regression analysis revealed that POR protein, as well as presence of the *CYP2C19*2A* variant, was a significant contributor to variability in the CYP2C19 activity in HLMs. POR activity would likely have been a better measure of POR function in supporting CYP2C19 reactions than microsomal POR protein concentration, particularly if there were intrinsic differences in the flavin content of the POR flavoprotein or if there was differential flavin loss during microsomal isolation and storage. However, because of limited availability of microsomes from many of the samples, we were unable to conduct comprehensive POR activity measurements. Working on the assumption that POR activity is dependent on POR protein content, we utilized the latter parameter in our multivariate analysis. If hepatic POR content can be linked to specific POR variants, testing for these variants may have utility for the individualization of clopidogrel therapy.

In conclusion, the present study revealed that both the *CYP2C19*2A* and *CYP2C19*17* alleles contributed to variability in hepatic CYP2C19 protein content and (S)-mephenytoin 4′-hydroxylase activity. However, only the *CYP2C19*2A* allele had a significant effect on clopidogrel and 2-oxo-clopidogrel metabolism, consistent with the multienzyme nature of these reactions. In addition, HLMs from donors with a *CYP2C19*2A/*17* diplotype exhibited (S)-mephenytoin 4′-hydroxylase activity most similar to that of HLMs for the *CYP2C19*1B/*2A* diplotype, consistent with the much stronger functional impact of the **2A* null allele. A substantial fraction of interliver differences in CYP2C19 activity was unexplained, but some of it could be attributed to variation in POR content. Potential sources for future investigation include variation in *CYP2C19* regulatory genes and other endogenous and exogenous environmental factors (for example, regulatory hormone levels, diet and stress metrics).

CONFLICT OF INTEREST

The authors declare no conflict of interest.

ACKNOWLEDGMENTS

This work was supported in part by grants from the National Institutes of Health (U01 GM092676 and GM092666, P01 GM32165 and R01 GM094418) and the Japan Society for the Promotion of Science Postdoctoral Fellowship for Research Abroad (H23-694) and The Uehara Memorial Foundation Research Fellowship (201340221) to Dr Shirasaka. We thank the Hartwell Center at St Jude Children's Research Hospital for sequencing DNA for this study.

REFERENCES

1 Li-Wan-Po A, Girard T, Farndon P, Cooley C, Lithgow J. Pharmacogenetics of CYP2C19: functional and clinical implications of a new variant CYP2C19*17. *Br J Clin Pharmacol* 2010; **69**: 222–230.
2 Shah BS, Parmar SA, Mahajan S, Mehta AA. An insight into the interaction between clopidogrel and proton pump inhibitors. *Curr Drug Metab* 2012; **13**: 225–235.
3 Shirasaka Y, Sager JE, Lutz JD, Davis C, Isoherranen N. Inhibition of CYP2C19 and CYP3A4 by omeprazole metabolites and their contribution to drug-drug interactions. *Drug Metab Dispos* 2013; **41**: 1414–1424.
4 Wedlund PJ. The CYP2C19 enzyme polymorphism. *Pharmacology* 2000; **61**: 174–183.
5 McGraw J, Waller D. Cytochrome P450 variations in different ethnic populations. *Expert Opin Drug Metab Toxicol* 2012; **8**: 371–382.
6 Hicks JK, Swen JJ, Thorn CF, Sangkuhl K, Kharasch ED, Ellingrod VL *et al.* Clinical Pharmacogenetics Implementation Consortium guideline for CYP2D6 and CYP2C19 genotypes and dosing of tricyclic antidepressants. *Clin Pharmacol Ther* 2013; **93**: 402–408.
7 De Morais SM, Wilkinson GR, Blaisdell J, Nakamura K, Meyer UA, Goldstein JA. The major genetic defect responsible for the polymorphism of S-mephenytoin metabolism in humans. *J Biol Chem* 1994; **269**: 15419–1522.
8 Ferguson RJ, De Morais SM, Benhamou S, Bouchardy C, Blaisdell J, Ibeanu G *et al.* A new genetic defect in human CYP2C19: mutation of the initiation codon is responsible for poor metabolism of S-mephenytoin. *J Pharmacol Exp Ther* 1998; **284**: 356–361.
9 Sim SC, Risinger C, Dahl ML, Aklillu E, Christensen M, Bertilsson L *et al.* A common novel CYP2C19 gene variant causes ultrarapid drug metabolism relevant for the

drug response to proton pump inhibitors and antidepressants. *Clin Pharmacol Ther* 2006; **79**: 103–113.
10 Sanford JC, Guo Y, Sadee W, Wang D. Regulatory polymorphisms in CYP2C19 affecting hepatic expression. *Drug Metabol Drug Interact* 2013; **28**: 23–30.
11 Furuta T, Ohashi K, Kosuge K, Zhao XJ, Takashima M, Kimura M *et al.* CYP2C19 genotype status and effect of omeprazole on intragastric pH in humans. *Clin Pharmacol Ther* 1999; **65**: 552–561.
12 Klotz U. Clinical impact of CYP2C19 polymorphism on the action of proton pump inhibitors: a review of a special problem. *Int J Clin Pharmacol Ther* 2006; **44**: 297–302.
13 Mega JL, Close SL, Wiviott SD, Shen L, Hockett RD, Brandt JT *et al.* Cytochrome p-450 polymorphisms and response to clopidogrel. *N Engl J Med* 2009; **360**: 354–362.
14 Mega JL, Simon T, Collet JP, Anderson JL, Antman EM, Bliden K *et al.* Reduced-function CYP2C19 genotype and risk of adverse clinical outcomes among patients treated with clopidogrel predominantly for PCI: a meta-analysis. *JAMA* 2010; **304**: 1821–1830.
15 Hwang SJ, Jeong YH, Kim IS, Koh JS, Kang MK, Park Y *et al.* The cytochrome 2C19*2 and *3 alleles attenuate response to clopidogrel similarly in East Asian patients undergoing elective percutaneous coronary intervention. *Thromb Res* 2011; **127**: 23–28.
16 Sibbing D, Koch W, Gebhard D, Schuster T, Braun S, Stegherr J *et al.* Cytochrome 2C19*17 allelic variant, platelet aggregation, bleeding events, and stent thrombosis in clopidogrel-treated patients with coronary stent placement. *Circulation* 2010; **121**: 512–518.
17 Tiroch KA, Sibbing D, Koch W, Roosen-Runge T, Mehilli J, Schömig A *et al.* Protective effect of the CYP2C19 *17 polymorphism with increased activation of clopidogrel on cardiovascular events. *Am Heart J* 2010; **160**: 506–512.
18 Paré G, Mehta SR, Yusuf S, Anand SS, Connolly SJ, Hirsh J *et al.* Effects of CYP2C19 genotype on outcomes of clopidogrel treatment. *N Engl J Med* 2010; **363**: 1704–1714.
19 Goldstein JA, Faletto MB, Romkes-Sparks M, Sullivan T, Kitareewan S, Raucy JL *et al.* Evidence that CYP2C19 is the major (S)-mephenytoin 4'-hydroxylase in humans. *Biochemistry* 1994; **33**: 1743–1752.
20 Baldwin RM, Ohlsson S, Pedersen RS, Mwinyi J, Ingelman-Sundberg M, Eliasson E *et al.* Increased omeprazole metabolism in carriers of the CYP2C19*17 allele; a pharmacokinetic study in healthy volunteers. *Br J Clin Pharmacol* 2008; **65**: 767–774.
21 Ohlsson Rosenborg S, Mwinyi J, Andersson M, Baldwin RM, Pedersen RS, Sim SC *et al.* Kinetics of omeprazole and escitalopram in relation to the CYP2C19*17 allele in healthy subjects. *Eur J Clin Pharmacol* 2008; **64**: 1175–1179.
22 Wang G, Lei HP, Li Z, Tan ZR, Guo D, Fan L *et al.* The CYP2C19 ultra-rapid metabolizer genotype influences the pharmacokinetics of voriconazole in healthy male volunteers. *Eur J Clin Pharmacol* 2009; **65**: 281–285.
23 De Vos A, van der Weide J, Loovers HM. Association between CYP2C19*17 and metabolism of amitriptyline, citalopram and clomipramine in Dutch hospitalized patients. *Pharmacogenomics J* 2011; **11**: 359–367.
24 Dolton MJ, McLachlan AJ. Clinical importance of the CYP2C19*17 variant allele for voriconazole. *Br J Clin Pharmacol* 2011; **71**: 137–138.
25 Gawrońska-Szklarz B, Adamiak-Giera U, Wyska E, Kurzawski M, Gornik W, Kaldonska M *et al.* CYP2C19 polymorphism affects single-dose pharmacokinetics of oral pantoprazole in healthy volunteers. *Eur J Clin Pharmacol* 2012; **68**: 1267–1274.
26 Lewis JP, Stephens SH, Horenstein RB, O'Connell JR, Ryan K, Peer CJ *et al.* The CYP2C19*17 variant is not independently associated with clopidogrel response. *J Thromb Haemost* 2013; **11**: 1640–1646.
27 Pedersen RS, Brasch-Andersen C, Sim SC, Bergmann TK, Halling J, Petersen MS *et al.* Linkage disequilibrium between the CYP2C19*17 allele and wildtype CYP2C8 and CYP2C9 alleles: identification of CYP2C haplotypes in healthy Nordic populations. *Eur J Clin Pharmacol* 2010; **66**: 1199–1205.
28 Anichavezhi D, Chakradhara Rao US, Shewade DG, Krishnamoorthy R, Adithan C. Distribution of CYP2C19*17 allele and genotypes in an Indian population. *J Clin Pharm Ther* 2012; **37**: 313–318.
29 Blaisdell J, Mohrenweiser H, Jackson J, Ferguson S, Coulter S, Chanas B *et al.* Identification and functional characterization of new potentially defective alleles of human CYP2C19. *Pharmacogenetics* 2002; **12**: 703–711.
30 Barrett JC, Fry B, Maller J, Daly MJ. Haploview: analysis and visualization of LD and haplotype maps. *Bioinformatics* 2005; **21**: 263–265.
31 Thummel KE, Kharasch ED, Podoll T, Kunze K. Human liver microsomal enflurane defluorination catalyzed by cytochrome P-450 2E1. *Drug Metab Dispos* 1993; **21**: 350–357.
32 Paine MF, Khalighi M, Fisher JM, Shen DD, Kunze KL, Marsh CL *et al.* Characterization of interintestinal and intraintestinal variations in human CYP3A-dependent metabolism. *J Pharmacol Exp Ther* 1997; **283**: 1552–1562.
33 Guengerich FP, Martin MV, Sohl CD, Cheng Q. Measurement of cytochrome P450 and NADPH-cytochrome P450 reductase. *Nat Protoc* 2009; **4**: 1245–1251.
34 Yamaoka K, Tanigawara Y, Nakagawa T, Uno T. A pharmacokinetic analysis program (multi) for microcomputer. *J Pharmacobiodyn* 1981; **4**: 879–885.
35 Korzekwa KR, Krishnamachary N, Shou M, Ogai A, Parise RA, Rettie AE *et al.* Evaluation of atypical cytochrome P450 kinetics with two-substrate models: evidence that multiple substrates can simultaneously bind to cytochrome P450 active sites. *Biochemistry* 1998; **37**: 4137–4147.
36 Omura T, Sato R. The carbon monoxide-binding pigment of liver microsomes. I. evidence for its hemoprotein nature. *J Biol Chem* 1964; **239**: 2370–2378.
37 Kamiie J, Ohtsuki S, Iwase R, Ohmine K, Katsukura Y, Yanai K *et al.* Quantitative atlas of membrane transporter proteins: development and application of a highly sensitive simultaneous LC/MS/MS method combined with novel in-silico peptide selection criteria. *Pharm Res* 2008; **25**: 1469–1483.
38 Prasad B, Unadkat JD. Optimized approaches for quantification of drug transporters in tissues and cells by MRM proteomics. *AAPS J* 2014; **16**: 634–648.
39 Edson KZ, Prasad B, Unadkat JD, Suhara Y, Okano T, Guengerich FP *et al.* Cytochrome P450-dependent catabolism of vitamin K: omega-hydroxylation catalyzed by human CYP4F2 and CYP4F11. *Biochemistry* 2013; **52**: 8276–8285.
40 Prasad B, Evers R, Gupta A, Hop CE, Salphati L, Shukla S *et al.* Interindividual variability in hepatic organic anion-transporting polypeptides and P-glycoprotein (ABCB1) protein expression: quantification by liquid chromatography tandem mass spectroscopy and influence of genotype, age, and sex. *Drug Metab Dispos* 2014; **42**: 78–88.
41 Solstad T, Bjørgo E, Koehler CJ, Strozynski M, Torgersen KM, Taskén K *et al.* Quantitative proteome analysis of detergent-resistant membranes identifies the differential regulation of protein kinase C isoforms in apoptotic T cells. *Proteomics* 2010; **10**: 2758–2768.
42 Kazui M, Nishiya Y, Ishizuka T, Hagihara K, Farid NA, Okazaki O *et al.* Identification of the human cytochrome P450 enzymes involved in the two oxidative steps in the bioactivation of clopidogrel to its pharmacologically active metabolite. *Drug Metab Dispos* 2010; **38**: 92–99.
43 Fukushima-Uesaka H, Saito Y, Maekawa K, Ozawa S, Hasegawa R, Kajio H *et al.* Genetic variations and haplotypes of CYP2C19 in a Japanese population. *Drug Metab Pharmacokinet* 2005; **20**: 300–307.
44 Gurbel PA, Tantry US, Shuldiner AR. Letter by Gurbel et al regarding article, "Cytochrome 2C19*17 allelic variant, platelet aggregation, bleeding events, and stent thrombosis in clopidogrel-treated patients with coronary stent placement". *Circulation* 2010; **122**: e478.
45 Hanioka N, Tsuneto Y, Saito Y, Sumada T, Maekawa K, Saito K *et al.* Functional characterization of two novel CYP2C19 variants (CYP2C19*18 and CYP2C19*19) found in a Japanese population. *Xenobiotica* 2007; **37**: 342–355.
46 Scott SA, Sangkuhl K, Gardner EE, Stein CM, Hulot JS, Johnson JA *et al.* Clinical Pharmacogenetics Implementation Consortium guidelines for cytochrome P450-2C19 (CYP2C19) genotype and clopidogrel therapy. *Clin Pharmacol Ther* 2011; **90**: 328–332.
47 Sibbing D, Gebhard D, Koch W, Braun S, Stegherr J, Morath T *et al.* Isolated and interactive impact of common CYP2C19 genetic variants on the anti-platelet effect of chronic clopidogrel therapy. *J Thromb Haemost* 2010; **8**: 1685–1693.
48 Qin XP, Xie HG, Wang W, He N, Huang SL, Xu ZH *et al.* Effect of the gene dosage of CgammaP2C19 on diazepam metabolism in Chinese subjects. *Clin Pharmacol Ther* 1999; **66**: 642–646.
49 Raucy JL, Mueller L, Duan K, Allen SW, Strom S, Lasker JM. Expression and induction of CYP2C P450 enzymes in primary cultures of human hepatocytes. *J Pharmacol Exp Ther* 2002; **302**: 475–482.
50 Foti RS, Wahlstrom JL. CYP2C19 inhibition: the impact of substrate probe selection on in vitro inhibition profiles. *Drug Metab Dispos* 2008; **36**: 523–528.
51 Moody GC, Griffin SJ, Mather AN, McGinnity DF, Riley RJ. Fully automated analysis of activities catalysed by the major human liver cytochrome P450 (CYP) enzymes: assessment of human CYP inhibition potential. *Xenobiotica* 1999; **29**: 53–75.
52 Furuta S, Kamada E, Suzuki T, Sugimoto T, Kawabata Y, Shinozaki Y *et al.* Inhibition of drug metabolism in human liver microsomes by nizatidine, cimetidine and omeprazole. *Xenobiotica* 2001; **31**: 1–10.
53 Ohyama K, Nakajima M, Suzuki M, Shimada N, Yamazaki H, Yokoi T. Inhibitory effects of amiodarone and its N-deethylated metabolite on human cytochrome P450 activities: prediction of in vivo drug interactions. *Br J Clin Pharmacol* 2000; **49**: 244–253.
54 Frye RF, Zgheib NK, Matzke GR, Chaves-Gnecco D, Rabinovitz M, Shaikh OS *et al.* Liver disease selectively modulates cytochrome P450--mediated metabolism. *Clin Pharmacol Ther* 2006; **80**: 235–245.
55 Stein DM, Lindell A, Murdock KR, Kufera JA, Menaker J, Keledjian K *et al.* Relationship of serum and cerebrospinal fluid biomarkers with intracranial

hypertension and cerebral hypoperfusion after severe traumatic brain injury. *J Trauma* 2011; **70**: 1096–1103.
56 Abdel-Razzak Z, Loyer P, Fautrel A, Gautier JC, Corcos L, Turlin B *et al*. Cytokines down-regulate expression of major cytochrome P-450 enzymes in adult human hepatocytes in primary culture. *Mol Pharmacol* 1993; **44**: 707–715.
57 Warren GW, van Ess PJ, Watson AM, Mattson MP, Blouin RA. Cytochrome P450 and antioxidant activity in interleukin-6 knockout mice after induction of the acute-phase response. *J Interferon Cytokine Res* 2001; **21**: 821–826.
58 Waxman DJ, Holloway MG. Sex differences in the expression of hepatic drug metabolizing enzymes. *Mol Pharmacol* 2009; **76**: 215–228.
59 Waxman DJ, O'Connor C. Growth hormone regulation of sex-dependent liver gene expression. *Mol Endocrinol* 2006; **20**: 2613–2629.

Supplementary Information accompanies the paper on the The Pharmacogenomics Journal website (http://www.nature.com/tpj)